AIAA JOURNAL
Vol. 32, No. 9, September 1994

Technical Notes

TECHNICAL NOTES are short manuscripts describing new developments or important results of a preliminary nature. These Notes cannot exceed 6 manuscript pages and 3 figures; a page of text may be substituted for a figure and vice versa. After informal review by the editors, they may be published within a few months of the date of receipt. Style requirements are the same as for regular contributions (see inside back cover).

Significance of Shock Structure on Supersonic Jet Mixing Noise of Axisymmetric Nozzles

Chan M. Kim* and Eugene A. Krejsa†
NASA Lewis Research Center, Cleveland, Ohio 44135
and
Abbas Khavaran‡
NYMA, Lewis Research Group, Brook Park, Ohio 44142

Introduction

ONE of the key technical elements in NASA's high speed research program is reducing the noise level to meet the federal noise regulation. The dominant noise source is associated with the supersonic jet discharged from the engine exhaust system. Whereas the turbulence mixing is largely responsible for the generation of the jet noise, a broadband shock-associated noise is also generated when the nozzle operates at conditions other than its design condition. For both mixing and shock noise components, because the source of the noise is embedded in the jet plume, one can expect that jet noise can be predicted from the jet flowfield computation. Mani et al.[1] developed a unified aerodynamic/acoustic prediction scheme by applying an extension of Reichardt's aerodynamic model[2] to compute turbulent shear stresses which are utilized in estimating the strength of the noise source. Although this method produces a fast and practical estimate of the jet noise, a modification by Khavaran et al.[3] has led to an improvement in aerodynamic solution. The most notable feature in this work is that Reichardt's model is replaced with the computational fluid dynamics (CFD) solution of Reynolds-averaged Navier-Stokes equations. The major advantage of this work is that the essential, noise-related flow quantities such as turbulence intensity and shock strength can be better predicted. The predictions in Ref. 3 were limited to a shock-free design condition and the effect of shock structure on the jet mixing noise was not addressed. The present work is aimed at investigating this issue. Under imperfectly expanded conditions the existence of the shock cell structure and its interaction with the convecting turbulence structure may not only generate a broadband shock-associated noise but also change the turbulence structure, and thus the strength of the mixing noise source. Failure in capturing shock structures properly could lead to incorrect aeroacoustic predictions.

Method of Solution

The solution technique to compute the noise field is essentially based on the methodology developed in Ref. 1, as modified in Ref. 3, and details are documented in Ref. 3. As mentioned earlier, a major modification was made such that Reichardt's aerodynamic model has been replaced with a CFD solution. This improvement, as shown in Ref. 3, not only eliminates some of the empiricism in the original method of Ref. 1 but also provides a better estimate of source strength and sound/flow interaction. More critically, for the imperfectly expanded jet flow conditions, a CFD solution can properly predict the shock structure which is not taken into account in Reichardt's model.

To compute the flowfield, the PARC code[4] with a k-ε turbulence model[5] was used. This code solves the complete Reynolds-averaged Navier-Stokes equations in conservative law form using the Beam and Warming approximate factorization algorithm and has been verified for a variety of aerodynamic problems. As far as dealing with shock structure goes, this code has a tendency to numerically attenuate downstream shocks. While the basic numerical schemes and turbulence modeling may be responsible for this attenuation problem, the effect of mesh size has not been addressed properly in the open literature. To investigate this issue and compare aerodynamic and acoustic results, convergent and convergent-divergent (CD), axisymmetric nozzle geometries were selected. These nozzles have the same equivalent diameter and both aerodynamic and acoustic test results have been reported in Ref. 6.

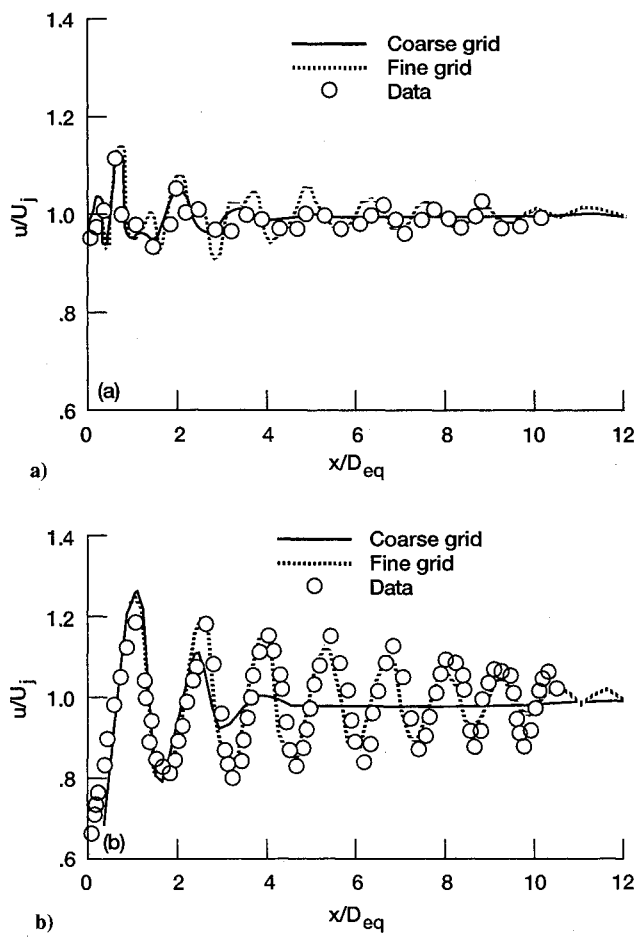

Fig. 1 Centerline axial velocity profile: a) CD nozzle, NPR = 3.312 and b) convergent nozzle, NPR = 3.323.

Presented as Paper 93-0735 at the AIAA 31st Aerospace Sciences Meeting, Reno, NV, Jan. 11–14, 1993; received Sept. 28, 1993; revision received Feb. 14, 1994; accepted for publication Feb. 16, 1994.

*Aerospace Engineer, Turbomachinery Technology Branch, MS 77-6, 21000 Brookpark Road.

†Deputy Branch Chief, Propeller and Acoustics Technology Branch. Member AIAA.

‡Senior Research Engineer. Member AIAA.

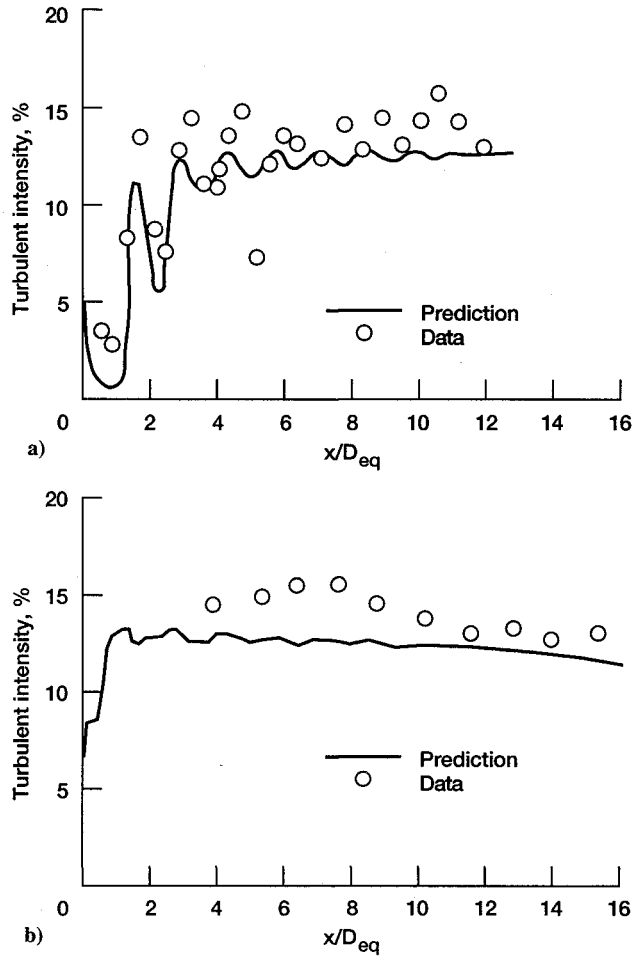

Fig. 2 Turbulent intensity profiles along the lipline: a) convergent nozzle and b) CD nozzle.

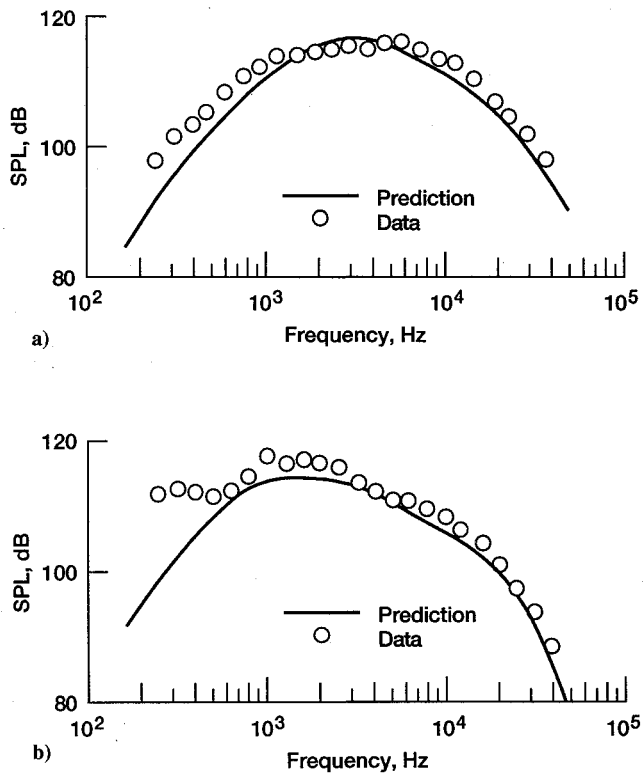

Fig. 3 Noise spectra for the convergent nozzle, NPR = 3.323: a) θ = 120 deg and b) θ = 160 deg.

Results and Discussion

The basic philosophy in studying the grid issue is that the grid size in a radial direction has little effect on resolving shock structures, and thus only the number of grids in the axial direction is varied. Figure 1a shows the centerline axial velocity profile for the CD nozzle operated at a nozzle pressure ratio (NPR) of 3.312. The design pressure ratio (DPR) for this nozzle is 3.121. Both coarse (141 × 61) and fine (441 × 61) grid solutions are depicted. Here U_j and D_{eq} correspond to the fully expanded jet exit velocity and the equivalent nozzle diameter, respectively. Although the shock strengths are relatively weak due to a slightly imperfectly ex-

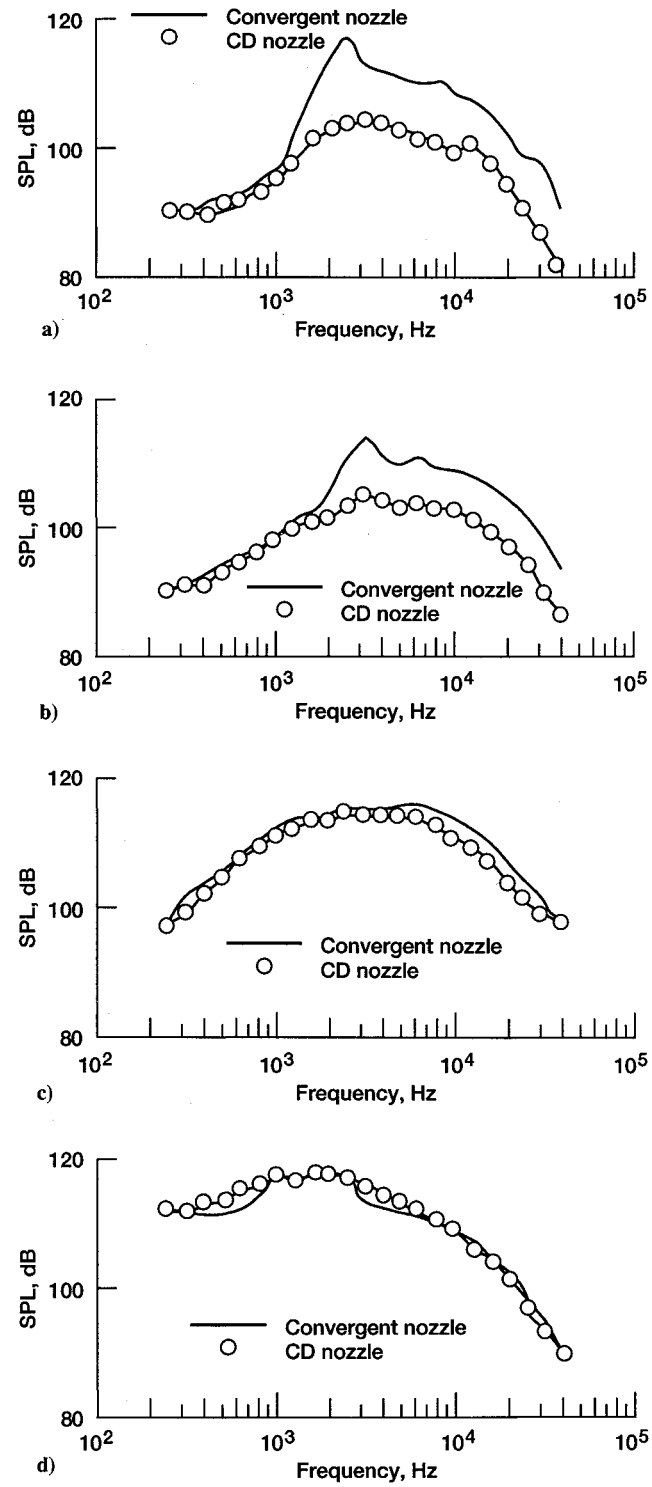

Fig. 4 Comparison of measured noise spectra between convergent nozzle and CD nozzle of same equivalent diameter at the same nozzle pressure of 3.3: a) θ = 60 deg, b) θ = 90 deg, c) θ = 120 deg, and d) θ = 160 deg.

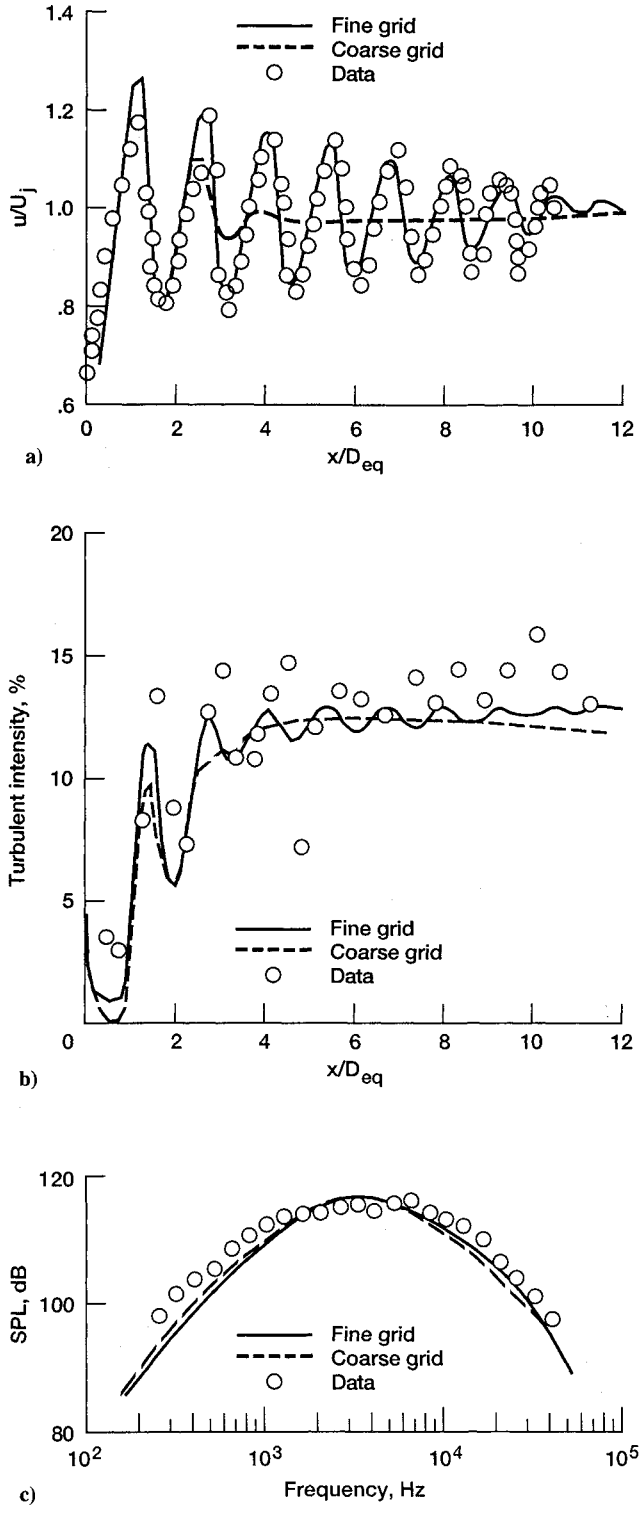

Fig. 5 Comparison of fine and coarse grid solutions with data for the convergent nozzle geometry, NPR = 3.323: a) centerline axial velocity profile, b) turbulent intensity profiles along the lipline, and c) noise spectrum at θ = 120 deg.

panded test condition, the fine grid solution exhibits a better capturing of the downstream shock structures. For the similar NPR of 3.323, the convergent nozzle geometry shows much stronger shock data as is shown in Fig. 1b. Here 141 × 71 and 421 × 71 grids were used for coarse and fine grid solutions, respectively. The predicted axial velocity profile along the centerline clearly shows that proper grid resolution is required for a better flowfield solution including shock structures. As explained earlier, the turbulence intensity is directly related to the strength of the mixing noise sources. Depicted in Fig. 2 are fine grid solutions of a turbulence intensity profile along the lipline compared with experimental data. The nozzle geometries and pressure ratios are the same as those mentioned earlier and a fair agreement with data is shown.

Based on the fine grid solutions of mean and turbulent quantities, one-third octave band sound pressure levels for the convergent nozzle geometry are compared with measured data at a 12.2-m radius in Fig. 3. Here θ is measured with respect to the upstream inlet axis. Only sound pressure levels in the rear quadrant region where the mixing noise is dominant are shown. Good agreement between prediction and data shows that the CFD-incorporated noise prediction scheme, which was demonstrated for the shock-free condition in Ref. 3, also works as well for shock-containing flow conditions. Similar comparisons were made for the CD nozzle geometry at an underexpanded (NPR = 3.312) and an overexpanded (NPR = 2.62) condition and a good agreement was achieved.

An interesting observation can be made by comparing the noise data between convergent and CD nozzles. Figure 4 shows measured noise data at several different observer angles for convergent and CD nozzle geometries operated at the same pressure ratio of 3.3. The equivalent diameter for two nozzles is the same here. It is obvious that the differences in spectra at angles of 60 and 90 deg are due to the shock noise contribution. Note that, for the same pressure ratio and the nozzle equivalent diameter, the mixing noise as observed at angles of 120 and 160 deg is almost identical. Considering the distinctive difference in the flowfield between the two nozzle geometries it appears that the mixing noise is almost independent of the shock strengths. This observation was also reflected in the prediction and provides an indication that the turbulence mixing noise is relatively insensitive to the variation of the shock structure.

Earlier, the effect of grid resolution on aerodynamic solution, especially the shock structure, was discussed. The question then naturally arises as to whether or not the noise is also affected by the grid resolution. To investigate this issue the test condition for the convergent nozzle geometry is considered. Depicted in Fig. 5 are the centerline axial velocity profile, lipline turbulent intensity, and the sound pressure level spectrum at 120 deg showing coarse and fine grid solutions. Despite the difference in mean flow quantities as represented by the centerline axial velocity profile in Fig. 5a the noise predictions exhibit little dependence on the grid resolution as is shown in Fig. 5c. This may be explained by the fact that the turbulent intensity distribution, which provides the estimate of the noise source strength, is about the same on the average between coarse and fine grid solutions as is shown in Fig. 5b. It should be noted, however, that proper capturing of shock structures is still very important from the viewpoint of the sound propagation where the mean flow gradients determine the radiation patterns. This is more crucial in computation of the broadband shock-associated noise which is generated by the interaction between the shock-cell structure and turbulence.

Conclusions

In this study the turbulent mixing noise generated by imperfectly expanded supersonic jets is computed and compared with experimental data. The noise computation is based on CFD-generated aerodynamic results using the PARC code and the acoustic prediction methodology described in Ref. 3. The nozzle geometry selected for the comparison consists of convergent and CD, axisymmetric nozzles. The effect of better grid resolution on capturing more accurate shock structures is investigated and demonstrated. Both aerodynamic and acoustic predictions agree well with measured data. Comparison of measured noise spectra between convergent and CD nozzles of the same equivalent diameter shows that, at the same nozzle pressure ratio, the mixing noise contribution is almost identical in spite of quite a difference in shock structures in the flowfield. The prediction also reveals the same observation, which implies that the turbulence mixing noise is barely affected by the shock strengths. Similar arguments hold for the effect of grid resolution on the noise prediction. Although the fine grid solution agrees much better with aerodynamic data, the mixing noise spectra show little difference between fine and coarse

grid noise predictions. This may not be true when it comes to incorporating the nonaxisymmetric nozzle geometry and sound/flow interaction where the mean flow gradients dominate the whole mechanism of sound radiation. Accurate prediction of the flowfield including the shock structure is more important in properly estimating the shock-associated noise.

References

[1]Mani, R., Balsa, T. E., Gliebe, P. R., Kantola, R. A., Stringes, E. J., and Wang, J. F. C., "High Velocity Jet Noise Source Location and Reduction," Task 2, Federal Aviation Administration, FAA-RD-76-79-II, Washington, DC, May 1978.

[2]Reichardt, H., "On a New Theory of Free Turbulence," *Royal Aeronautical Society Journal*, Vol. 47, June 1943, pp. 167–176.

[3]Khavaran, A., Krejsa, E. A., and Kim, C. M., "Computation of Supersonic Jet Mixing Noise for an Axisymmetric CD Nozzle Using k-ε Turbulence Model," AIAA Paper 92-0500, Jan. 1992.

[4]Cooper, G. K., and Sirbaugh, J. R., "PARC Code: Theory and Usage," Arnold Engineering Development Center, AEDC-TR-89-15, Tullahoma, TN, Nov. 1989.

[5]Chien, K. Y., "Prediction of Channel and Boundary Layer Flows with a Low Reynolds-Number Turbulence Model," *AIAA Journal*, Vol. 20, No. 1, 1982, pp. 33–38.

[6]Yamamoto, K., Brausch, J. F., Janardan, B. A., Hoerst, D. J., Price, A. O., and Knott, P. R., "Experimental Investigation of Shock-Cell Noise Reduction for Single Stream Nozzles in Simulated Flight Comprehensive Data Report," NASA CR-168234, May 1984.

Diverging Solutions of the Boundary-Layer Equations near a Plane of Symmetry

Hans Thomann*
Swiss Federal Institute of Technology, 8092 Zurich, Switzerland

Introduction

EXPERIMENTS with converging and diverging turbulent boundary layers near a plane of symmetry are described by Pompeo et al.[1] The test section used to generate the boundary layers on the plane $y = 0$ is shown in Fig. 1. The experiments were compared with computations based on a finite-difference boundary-layer code by Bettelini.[2] The prediction of the diverging flow agreed fairly well with the measurements and posed no special problems. The prediction of the converging flow, on the other hand, was very difficult. The results were very sensitive to the choice of parameters, and diverging solutions were observed for some combinations of parameters. It is the purpose of the present paper to investigate this tendency with different methods. Cases 1 and 2 are based on integral methods for laminar flow as described by Eichelbrenner.[3] In case 1 the crossflow satisfies only the corresponding boundary condition at the wall which leads to a simple equation for the growth of the boundary-layer thickness. In case 2 the crossflow momentum equation is also taken into account, and case 3 uses Bettelini's code.[2] All three methods show that there exists a critical crossflow intensity beyond which the boundary-layer thickness $\delta(x)$ diverges at some x_s in the test section, and the same holds true also for turbulent flow. The results of case 1 and case 2 show that the skin friction vanishes at x_s. This divergence can, therefore, be called separation. However, it is a very peculiar case as no pressure gradient exists that could decelerate the x component of the flow. A similar situation exists in the plane of symmetry of a cone at angle of attack. Moore[4] observed that the diverging flow on the windward side of cone posed no problems whereas the converging flow on the leeward side became undetermined before separation of the crossflow took place. Boericke[5] observed similar problems when using a finite-difference code. The flow on the leeward side of a blunted cone, as investigated by Der,[6] is very similar to the present case. "Separation" is observed in both cases in spite of a vanishing axial pressure gradient. Good surveys of the state of the art are given by Refs. 3 and 7–9.

Received Jan. 24, 1994; revision received April 8, 1994; accepted for publication April 11, 1994.

*Professor, Department of Mechanical Engineering.

Assumptions and Equations

The external velocity field near the plane of symmetry ($z = 0$) was based on experiments of Pompeo et al.,[1] namely, $w_e(x, \delta, z) = w_z(x) \cdot z$ and $u_e(x, \delta, z) = U + w_{zx}(x) \cdot z^2/2$ with

$$w_z(x) = A \cdot \exp[(x - x_0)^2/B] \qquad w_{zx} = \frac{dw_z}{dx}$$

For the converging flow good approximations are $A = -31.4\ s^{-1}$, $B = 0.231\ m^2$, and $x_0 = 1$ m. The boundary layer was assumed to start at $x = -0.5$ m and to end at $x = 2.5$ m. Figure 7 in Pompeo et al.[1] and w_z are comparable.

The velocity components near the plane of symmetry can be written as

$$u = u_0(x, y) + u_1(x, y) \cdot z + \cdots$$

$$v = v_0(x, y) + v_1(x, y) \cdot z + \cdots$$

$$w = w_1(x, y) \cdot z + \cdots$$

Introducing these equations into the boundary-layer equations leads to the following expressions valid in the plane of symmetry near $z = 0$.

$$\frac{\partial u_0}{\partial x} + \frac{\partial v_0}{\partial y} + w_1 = 0 \tag{1}$$

$$u_0 \frac{\partial u_0}{\partial x} + v_0 \frac{\partial u_0}{\partial y} - \nu \frac{\partial^2 u_0}{\partial y^2} = 0 \tag{2}$$

$$u_0 \frac{\partial w_1}{\partial x} + v_0 \frac{\partial w_1}{\partial y} + w_1^2 - \nu \frac{\partial^2 w_1}{\partial y^2} = U w_{zx} + w_z^2 = S(x) \tag{3}$$

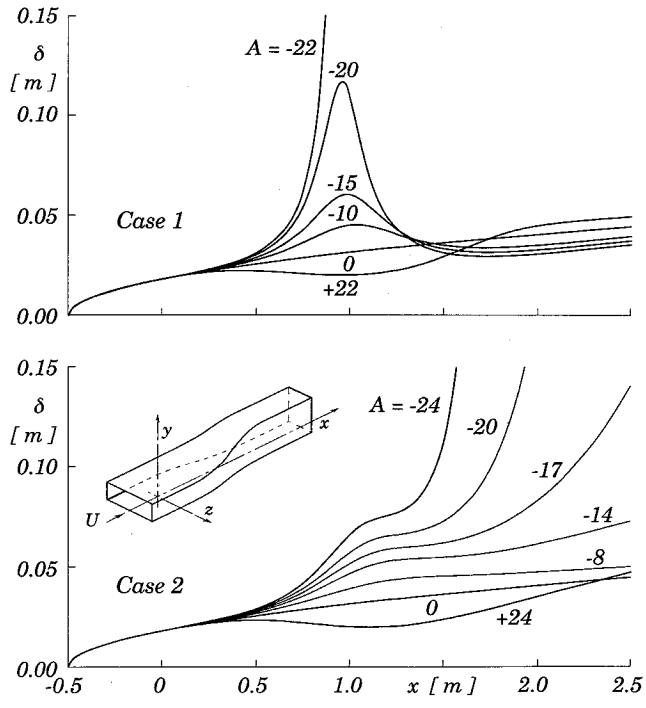

Fig. 1 Test section and boundary-layer thickness $\delta(x)$.